A *W*-Band Dielectric-Lens-Based Integrated Monopulse Radar Receiver

Sanjay Raman, *Member, IEEE*, N. Scott Barker, *Student Member, IEEE*, and Gabriel M. Rebeiz, *Fellow, IEEE*

***Abstract*—An integrated monopulse radar receiver has been developed for tracking applications at W-band frequencies. The receiver is based on dielectric-lens-supported, coplanar-waveguide-fed slot-ring antennas integrated with $\times 2$ uniplanar subharmonic mixers. The slot-ring antenna is capable of supporting two orthogonal modes offering the possibility of dual/multiple receive polarizations. The design center frequency is 94 GHz and the IF bandwidth is 2–4 GHz. The measured DSB conversion losses of the individual receiver channels range from 14.4 to 14.7 dB at an LO frequency of 45.0 GHz and an IF of 1.4 GHz. This includes the lens reflection and absorption losses, backside radiation, RF feedline loss, mixer conversion loss, and IF distribution loss. Excellent monopulse patterns are achieved with better than 45 dB difference pattern nulls using IF monopulse processing. This translates to submilliradian angular accuracy for a 24 mm aperture. Better than 25-dB nulls are possible over a 600-MHz bandwidth. The receiver is robust with respect to RF frequency.**

***Index Terms*— Antenna arrays, millimeter-wave technology, receivers.**

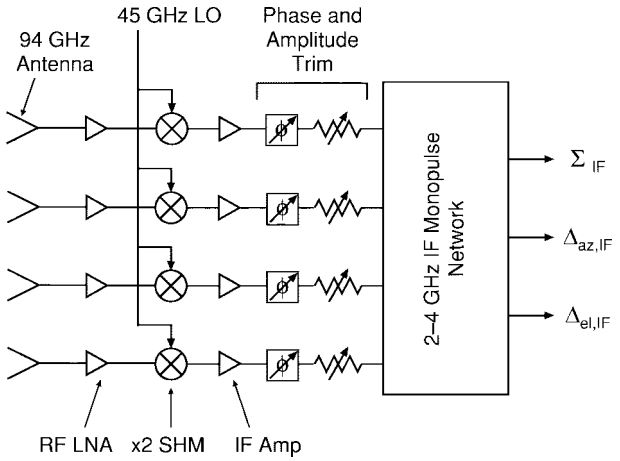

Fig. 1. Schematic of a four antenna monopulse receiver with subharmonic downconversion and IF processing.

I. Introduction

MILLIMETER-WAVE monopulse radars are attractive for high-resolution tracking applications such as antimissile munition terminal guidance and communications satellite tracking. In particular, narrow beamwidths for high angular accuracy are possible with a relatively small aperture size. For such systems, an integrated circuit approach, consisting of planar antennas directly integrated with RF (MMIC) electronics, offers the possibility of more compact, lower-cost front ends compared to waveguide-based alternatives. A potential problem which arises in millimeter-wave IC's and integrated antennas is that of *substrate modes*. In order to avoid power loss into these modes, very thin substrates (less than $\sim 0.1\lambda_d$) are typically required. Several planar and quasi-planar W-band monopulse systems have been demonstrated to date using various antenna geometries to minimize substrate losses, as well as different monopulse processing configurations [1]–[5].

A novel monopulse architecture based on micromachined integrated horn antennas (planar dipole antennas suspended on thin dielectric membranes to eliminate substrate moding) [5] performed the monopulse processing in the IF versus the RF. A schematic of a monopulse receiver with IF processing is shown in Fig. 1. In a planar millimeter-wave system, IF processing can provide much deeper nulls (in excess of 35 dB) due to the ability to phase and amplitude trim the four input channels prior to the monopulse network. Moreover, losses in a planar RF monopulse (which could be in excess of 2–3 dB at 94 GHz) will degrade the system noise figure; it is generally impractical to insert RF low-noise amplifiers (LNA's) prior to the planar comparator circuit.

A convenient method for eliminating substrate modes is to place a CPW-fed slot-type antenna on a dielectric lens of roughly the same dielectric constant as the antenna wafer [6]. The lens appears as a dielectric half-space, and hence does not support surface waves. Furthermore, the antenna radiates preferentially into the dielectric, resulting in high-directivity patterns. The dielectric lens system (fed with double-slot antennas) has been extensively analyzed by Filipovic *et al.* [7]. This approach was also utilized in a 35-GHz monopulse system based on slot-ring balanced mixers with polarization duplexed RF/LO [8].

In this paper, *CPW-fed* slot-ring antennas [9] are integrated with uniplanar subharmonic mixers [10] pumped with an on-chip LO to realize a W-band monopulse receiver. RF LNA's can be easily incorporated into the front-end and the need for quasi-optical LO injection is eliminated. Subharmonic mixing is utilized due to the relative ease of LO distribution at $\sim$45 GHz, and the inherent RF/LO isolation, which is important

Manuscript received March 30, 1998; revised August 28, 1998. This work was supported by the Naval Surface Warfare Center, Dahlgren Division, and by the Army Research Office under Contract DAAH04-94-G-0352 and Contract DAAH04-96-1-0348.

S. Raman is with The Bradley Department of Electrical and Computer Engineering, Virginia Polytechnic Institute and State University, Blacksburg, VA 24061-0111 USA.

N. S. Barker and G. M. Rebeiz are with The Radiation Laboratory, Electrical Engineering and Computer Science Department, The University of Michigan, Ann Arbor, MI 48109-2122 USA.

Publisher Item Identifier S 0018-9480(98)09203-5.

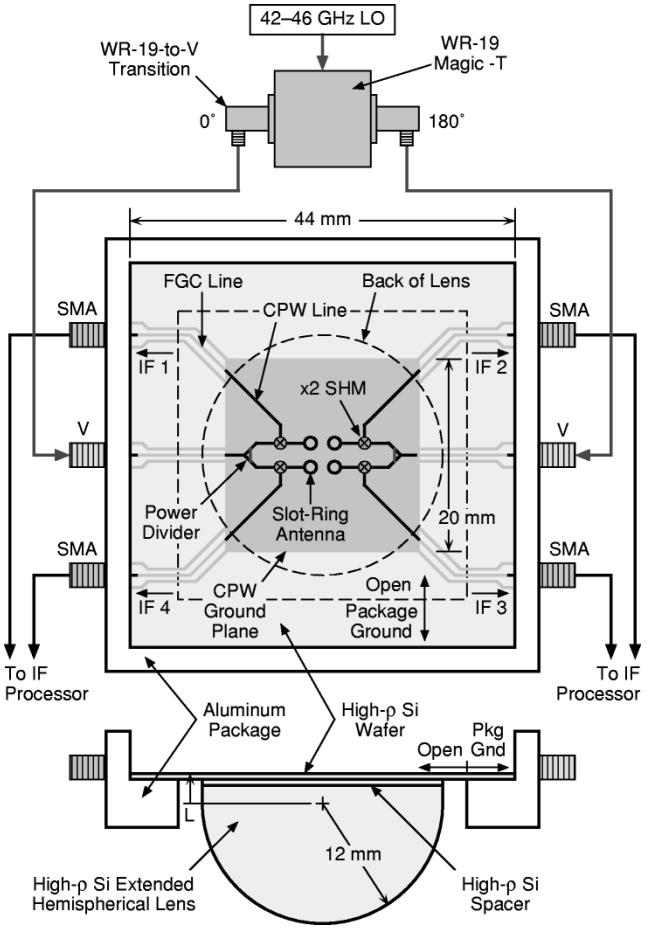

Fig. 2. Schematic of the W-band monopulse receiver, package, and LO source. $L = 4400$ μm. The packaged receiver is shown approximately to scale. The front-end electronics and LO/IF distribution circuits are integrated on a single 44 mm $\times$ 44 mm high-ρ silicon chip. The CPW ground plane area directly over the lens is 20 mm $\times$ 20 mm.

(in the absence of a front-end LNA) in order to minimize the leakage of LO power to the antennas.

II. Monopulse Receiver Design and Fabrication

A schematic of the receiver design is shown in Fig. 2. The design frequency is 94 GHz with an IF bandwidth of 2–4 GHz. A 2 $\times$ 2 array of slot-ring antennas is centered on the back side of a 24-mm-diameter dielectric lens at an extension length $L = 4400$ μm (the synthesized elliptical position) [9]. The center-to-center spacing of the slot-ring elements is chosen to be $0.8\lambda_d$ (746 μm) in order to avoid grating lobes while minimizing the effects of mutual coupling. The slot-ring antennas have a resonant input impedance of approximately 120 Ω. The RF signal received by each antenna is coupled to a uniplanar subharmonic mixer (labeled $\times$ 2 SHM in Fig. 2) via a 74 Ω CPW quarter-wave matching section which provides a -20 dB return loss over a 4% bandwidth in a 50 Ω system. Details of the mixer design are given in [10]; the mixer is based on University of Virginia SC1T7-D20 GaAs antiparallel Schottky diodes. A simple single-stub matching network at the LO port, consisting of a 75-Ω 63° (at 45.5 GHz) straight section and a 63.5-Ω 50° (at 45.5 GHz) open-circuited shunt stub, is utilized to improve the LO power performance.

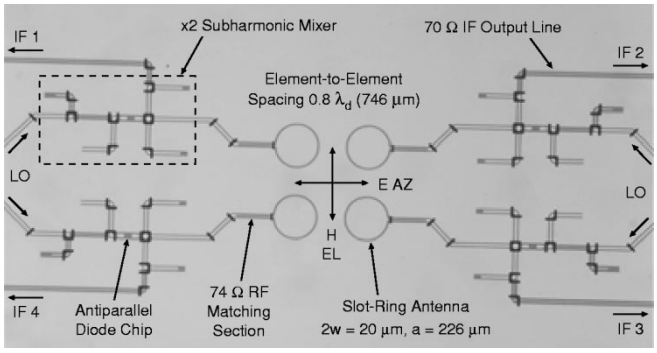

Fig. 3. Photograph of the fabricated slot-ring monopulse receiver. The LO Wilkinson power dividers are just out of the picture to the right and left.

The fabricated monopulse receiver chip is shown in Fig. 3. The receiver size excluding IF and LO distribution lines is 2.7 mm $\times$ 8.7 mm. Airbridges are included at various points in the circuit, particularly junctions, to suppress excitation of the undesired slotline (even) mode in the CPW line. The circuit was fabricated on 535-μm-thick high-resistivity (>2000 $\Omega\cdot$ cm) silicon with a 3000 Å PECVD-grown Si_xN_y layer (which is subsequently etched from the CPW gaps to avoid excessive line losses [10]). The bent sections in the RF feed lines are necessary to separate the mixer circuits by a reasonable spacing. The CPW center conductors and ground planes are 1.3-μm-thick evaporated Ti–Al–Ti–Au, which corresponds to 5 skin-depths at 94 GHz, and 3.5 skin-depths at 45.5 GHz. The 24-μm-wide airbridges are 3-μm-thick electroplated gold at a height of 3.5 μm above the CPW line. The 75 μm $\times$ 195 μm $\times$ 38 μm thick antiparallel diode chip is mounted using flip-chip technology and is bonded to the circuit using EPO-TEK H20E silver epoxy.[1] The design can be readily extended to a fully monolithic implementation.

The receiver chip is mounted in an aluminum package such that the periphery of the circuit exists over the package ground plane. For this reason, the LO input lines and the IF output lines transition from standard ungrounded CPW to finite ground coplanar (FGC) lines in order to eliminate the excitation of parallel plate modes between the CPW gound planes and the package ground [11]. The FGC lines transition to spark-plug-type coaxial connectors at the package walls using a straightforward CPW-to-coaxial transition [12]; the LO inputs are V-connectors[2] and the IF outputs are SMA connectors.

The LO source is a 42–46-GHz Gunn oscillator with WR-19 waveguide output. The LO signal is delivered to the receiver via a WR-19 Magic-T, WR-19-to-V-connector transitions, and V-connector cables. The Gunn source is connected to the Δ port of the Magic-T such that the colinear ports are 180° out-of-phase with each other; this is necessary since the left and right antenna pairs receive the LO from opposite directions on the receiver chip. The ~45-GHz LO signals are divided again on the receiver chip using CPW Wilkinson power dividers. A photograph of a fabricated CPW LO power divider test circuit is shown in Fig. 4. One of the power divider output ports (port

[1] EPO-TEK H20E is a product of Epoxy Technology, Inc., Billerica, MA.

[2] V-connector is a registered trademark of Wiltron Company, Morgan Hill, CA.

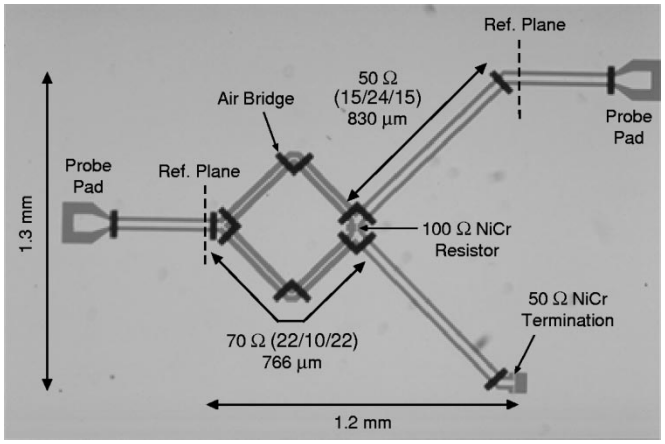

Fig. 4. Photograph of the fabricated CPW LO Wilkinson power divider test structure.

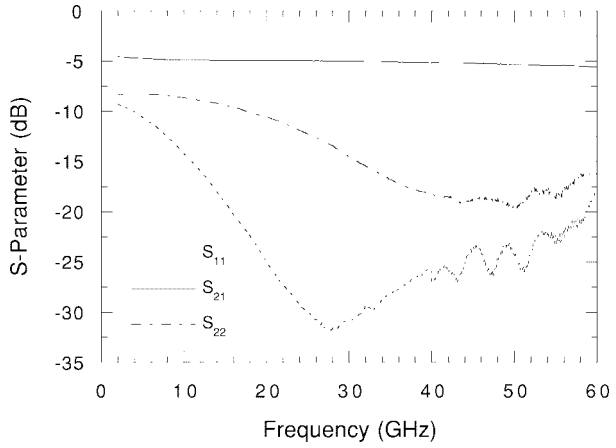

Fig. 5. Measured S-parameters of the CPW LO Wilkinson power divider test structure.

3) is terminated with a 50-Ω load consisting of two 100-Ω nickel–chrome (NiCr) thin-film resistors in parallel across the CPW gaps. The termination has a return loss of 29 dB at 45.5 GHz, and better than 25-dB return loss over the 2–60-GHz measurement band.

The measured S-parameters with respect to the indicated reference planes are shown in Fig. 5. The minimum value of S_{11} occurs at approximately 28 GHz; nonetheless, the return loss at 45 GHz is better than 23 dB. The divider demonstrates an insertion loss of 5.2 dB around 45.0 GHz. However, this includes an 830-μm-long section of 50-Ω CPW line necessary to connect to the mixer LO port in the 2×2 monopulse array configuration. The measured attenuation of the $w = 24$ μm, $g = 15$ μm CPW line is 4.6 dB/cm at 45.0 GHz, resulting in 0.4-dB loss in this additional line section. This indicates that the insertion loss through divider itself is approximately 4.8 dB at 45.0 GHz, of which 3 dB is the inherent power split of the divider. The additional 1.8 dB of loss is primarily due to the choice of CPW line dimensions in the divider; the loss can be reduced by using a larger $w + 2g$. The dimensions of the current design were selected to minimize the effects of the multiple bends and junctions in the divider circuit—in retrospect the design choice was overly conservative. The isolation of the power divider (S_{32}) was not measured due to lack of space on the layout for the additional two-port test structure required for this measurement.

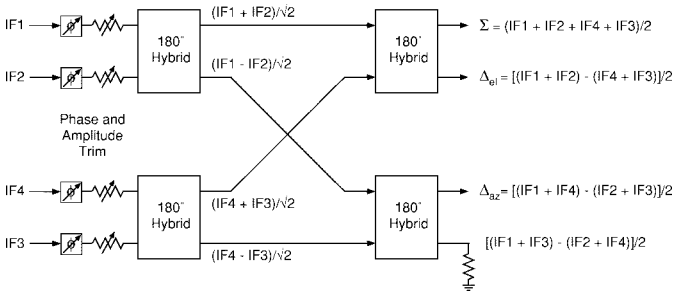

Fig. 6. IF monopulse comparator using 180° hybrids. IF1–IF4 represent the output signals from the monopulse receiver as shown in Fig. 2.

The IF monopulse comparator is the standard combination of 180° hybrids [13], and is preceded by SMA line-stretchers and variable attenuators for phase and amplitude trim (see Fig. 6). The diagonal difference port is terminated with an SMA 50-Ω load.

III. Measurements

A. Conversion Loss and Video Detection

Double sideband (DSB) conversion loss measurements were performed using the Y-factor method. Microwave absorber (ECCOSORB VHP-2-NRL)[3] at room temperature (290 K) or immersed in liquid nitrogen (77 K) provided the hot/cold load. The output of a given receiver channel was connected to a 1.4-GHz IF chain with a gain of 92 dB, a noise temperature of 68K, and a bandwidth of 50 MHz. The first stage of the IF chain was an isolator which directed any IF reflection to a cold termination. The measurements represent the conversion loss from a plane at the lens surface to the IF SMA connector, and the LO power is defined at the LO V-connector (see Fig. 2).

The DSB conversion loss of a typical channel centered on the back of the lens versus LO power and frequency is shown in Fig. 7. The minimum DSB conversion loss is 14.5 dB at an available LO power of 15–16 dBm at 45.0 GHz. The conversion loss levels do not vary significantly over the 44.5–46.0-GHz LO frequency range.

The measured data includes lens reflection (2.7 dB) and absorption (1.9 dB) losses, backside radiation (0.2 dB), RF feedline loss (1.0 dB), DSB mixer conversion loss (5 dB) [10], and IF losses from the mixer through the SMA connector. The IF line loss from the mixer output port to the FGC-to-coaxial-connector transition is estimated from measured TRL data to be 1.4 dB; the loss in the transition to the SMA connector is not known. A breakdown of these losses at an RF of 91 GHz are given in Table I; the quarter-wave RF matching section is assumed to contribute an additional 0.2 dB loss, and the IF connector transition is assumed to contribute an additional 0.5 dB loss. With the incorporation of an optimal matching cap layer on the lens, the reflection loss can be reduced by approximately 1.5 dB [7]. Reduction of the lens absorption

[3]ECCOSORB VHP-2-NRL is a product of Emerson and Cuming, Canton, MA.

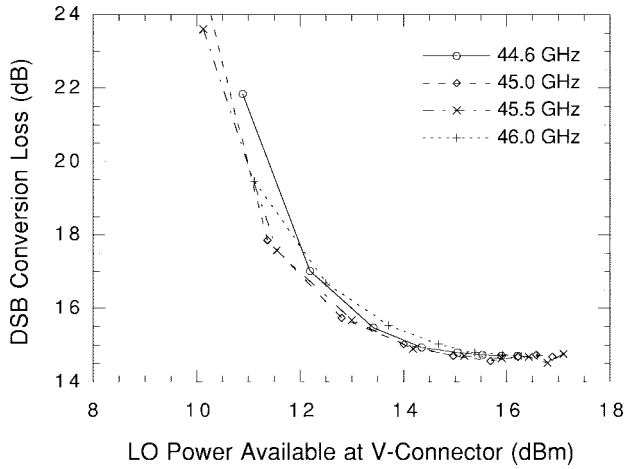

Fig. 7. Measured DSB conversion loss of channel #3 centered on the lens at the synthesized elliptical position ($L = 4400\ \mu$m) versus LO Power and frequency at an IF of 1.4 GHz.

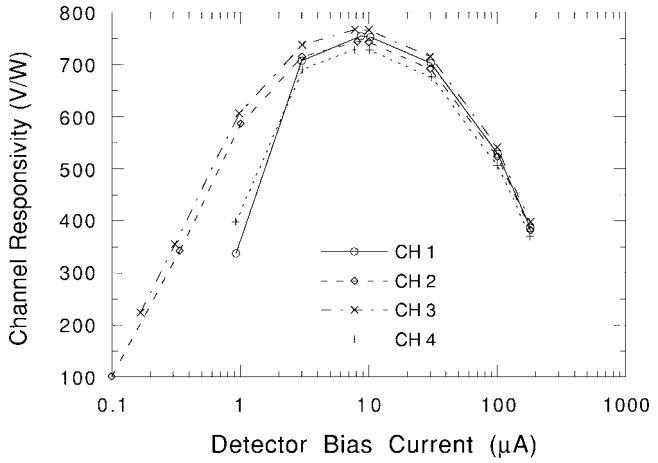

Fig. 8. Channel video responsivities, with 24-mm-diameter extended hemispherical silicon lens ($L = 4400\ \mu$m) centered on each individual channel, at 94 GHz.

TABLE I
MONOPULSE RECEIVER ANTENNA AND RF/IF FEEDLINE LOSS MECHANISMS AT $f_{RF} = 91$ GHz, IF = 1.4 GHz (24 mm HIGH-ρ Si LENS, $L = 4400\ \mu$m)

Calculated Lens Reflection Loss	2.7 dB
Estimated Lens Absorption Loss	1.9 dB
Calculated Backside Radiation	0.2 dB
Measured RF Feedline Loss[a]	1.2 dB
Estimated Mixer DSB Conversion Loss	5 dB
Measured IF Output Line Loss	1.4 dB
Assumed IF Connector Transition Loss	0.5 dB
Total	12.9 dB

[a] Includes 0.2 dB loss assumed for the quarter-wave RF matching section.

loss would require using a lower-loss material, such as semi-insulating GaAs.

The power loss in LO path at 45 GHz includes connector and transition loss (0.8 dB), CPW/FGC line loss (3.3 dB), and the Wilkinson power divider (5.2 dB), resulting in an estimated total loss of 9.3 dB from the input of the V-connector to the LO port of the mixer. Therefore, the estimated LO power at the LO port of each mixer for minimum receiver conversion loss is approximately 6–7 dBm.

Based on the above RF/IF losses, the total DSB conversion loss is expected to be approximately 13 dB, which is 1.5 dB lower than the measured value of 14.5 dB. It is not clear why the conversion loss is degraded by this amount, but possible contributing factors may be: 1) slightly increased RF losses in the mixer circuit due to a higher CPW line attenuation, as well as errors in the electrical lengths of the distributed elements due to the deviation from the design value of ϵ_{eff}, arising from variations in the PECVD Si_xN_y layer composition from that of the layer used in [10]; 2) additional loss and/or mismatch in the quarter-wavelength RF matching network for similar reasons; and 3) unforseen variations in the mixer RF input impedance without the RF bandpass filter used in [10].

Assuming a total front-end loss of 7.5 dB ($T_{eq} = 1340$ K), a DSB mixer conversion loss of 5 dB ($T_{eq} = 625$ K), and an IF output loss of 1.9 dB ($T_{eq} = 160$ K), the incorporation of an LNA with 26 dB gain and 4 dB NF ($T_N = 440$ K) [14] prior to the mixer circuit will result in an overall receiver conversion gain of 11.6 dB and a receiver noise temperature of 3830 K (a factor of 2 improvement over the measured value). RF LNA's are necessary to mitigate the mixer conversion loss and the back-end IF loss in order to realize lower noise operation.

To align the lens to the center of the 2×2 *array*, the video responsivity of each *individual channel* centered on the lens was first measured. The RF source was a W-band Gunn diode oscillator (chopped at 1 kHz) with a WR-10 standard gain pyramidal horn at the output. The receiver mount was located in the far field of the horn. The channel responsivity is defined as the detected low-frequency voltage, V_{detected}, across a 106-kΩ load (measured using a lock-in amplifier) per unit plane wave power incident on the entire lens area, and is given by

$$R_{\text{channel}} = \frac{V_{\text{detected}}}{S_{\text{incident}} \cdot A_{\text{phys}}} \tag{1}$$

where S_{incident} is the incident power density and A_{phys} is the physical area of the lens aperture. The video responsivities of the four individual channels are shown in Fig. 8. The deviation in the video responsivity for channels 1 and 4 at bias currents below approximately 3 μA is due to leakage currents which were noted in the I–V curve after diode mounting; in this case it is believed that these leakage currents are due to residue from the silver epoxy hardener, since the pad-to-pad I–V showed no indication of substrate leakage. The four channels had near-identical video responsivities at a bias current of 100 μA. With the receiver mount at its physical boresight, the lens position was adjusted until the detected signals from the four channels were equalized.

Then, with the lens aligned to the center of the *array*, the DSB conversion loss of each channel was measured with the maximum LO power available from the source setup in Fig. 2. The four channels had conversion losses within 0.3 dB of each other (14.4–14.7 dB) at an LO frequency of 45.0 GHz.

B. Monopulse Patterns and Null Bandwiths

The setup for measuring the monopulse antenna patterns and the difference pattern null depths is shown in Fig. 9.

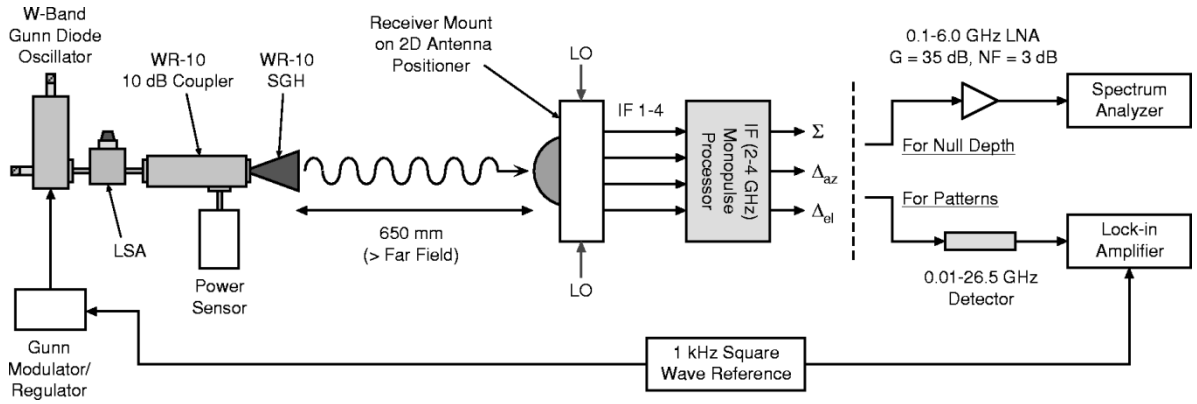

Fig. 9. Measurement setup for monopulse antenna patterns and accurate determination of null depth.

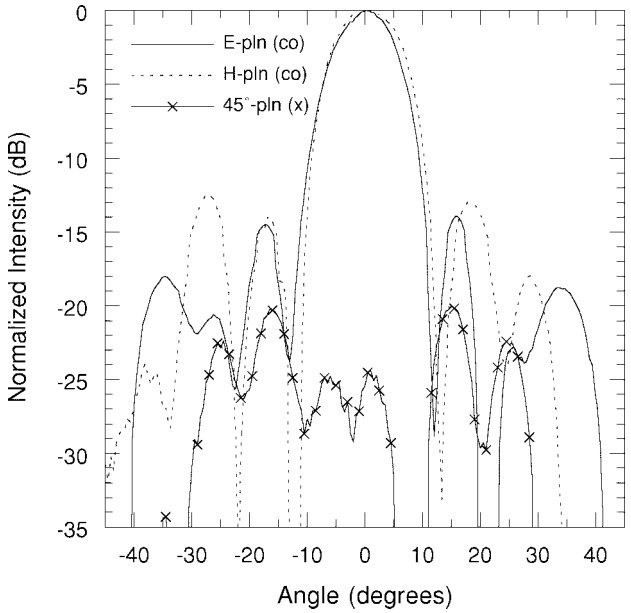

Fig. 10. Measured Σ port copolarized E- and H-plane patterns, and cross-polarized 45°-plane patterns at RF $=$ 93 GHz, IF $=$ 3 GHz.

For a given output port measurement at the IF comparator, the two idle ports are terminated with SMA 50-Ω loads. The monopulse patterns were measured by shining a W-band plane wave (chopped at 1 kHz) on the 24-mm receiver lens aperture, detecting the sum and difference outputs of the comparator, and measuring the detected low-frequency voltage with a lock-in amplifier. The receiver mount was scanned in the planes of interest with an automated 2-D antenna positioner in order to measure the monopulse patterns. The definitions of the principal pattern planes with respect to the slot-ring antenna array are shown in Fig. 3.

Fig. 10 shows the sum (Σ) port E- and H-plane copolarized patterns and the 45°-plane cross-polarized pattern at RF $=$ 93 GHz and IF $=$ 3 GHz. The sum pattern is rotationally symmetric, and exhibits a 12.5° 3-dB beamwidth, a 25° first null beamwidth, and cross-polarization levels below -25 dB in the main beam. These beamwidths are wider than the individual slot-ring antenna patterns with an identical lens geometry [9] since the sum pattern is literally the sum of the individual off-axis scanned beams for the four antennas. The relatively high sidelobe levels (-13 to -15 dB) are believed to be due to the receiver package and mounting structure.

The null depths were measured using a spectrum analyzer to accurately determine the *difference*-peak-to-null ratios at the IF comparator difference ports. The spectrum analyzer was preceded by a 0.01–6.0-GHz low-noise amplifier with 35-dB gain and a 3-dB noise figure to improve the dynamic range of the measurement. The monopulse comparator phase trimmers were initially adjusted to achieve the deepest possible null at RF $=$ 93 GHz and IF $=$ 3 GHz. A significant phase adjustment to channels 1 and 4 (relative to channels 2 and 3) was necessary to maximize the difference nulls on boresight; this is clearly due to a net phase difference between the two sides of the LO distribution after the power split in the waveguide Magic-T (Fig. 2). Amplitude adjustment proved to be unnecessary, as was expected since the four receiver channels have very well matched conversion losses. Fig. 11(a) shows the measured Σ E-plane and Δ_{az} patterns, and Fig. 11(b) shows the measured Σ H-plane and Δ_{el} patterns. The difference patterns were measured using the lock-in amplifier as discussed above except that the null depth was resolved using the spectrum analyzer. Better than 45-dB null depths (relative to the *difference pattern peak*) were achieved; this translates to submilliradian accuracy for a 24-mm aperture.

Fig. 12 presents the null depths versus IF frequency with $f_{\rm LO} = 45.0$ GHz and the monopulse comparator tuned for the deepest possible boresight null at IF $=$ 3 GHz. Measurements were performed initially with an excessive RF power level delivered to the diodes ($\sim$1 mW); at this power level only 30–40 dB nulls were realized. The null bandwidth measurements were then reperformed with a much lower power level ($\sim$4 μW) allowing $>$45-dB null depths to be resolved. However, the ripple in the curves was not eliminated by reducing the RF power level. This ripple is most likely due to a slight standing wave between the WR-10 transmit horn and the receiver mount (Fig. 9); indeed the ripple occurs approximately on a 200–250-MHz frequency scale, which roughly corresponds to a wavelength which could resonate in the 650-mm space between the transmit horn and the receiver. This problem could be eliminated by improving the absorber placement on the face of the receiver mount, or by increasing the distance between the transmitter and receiver. The standing wave did not have any apparent effect on the peaks of the sum and difference patterns.

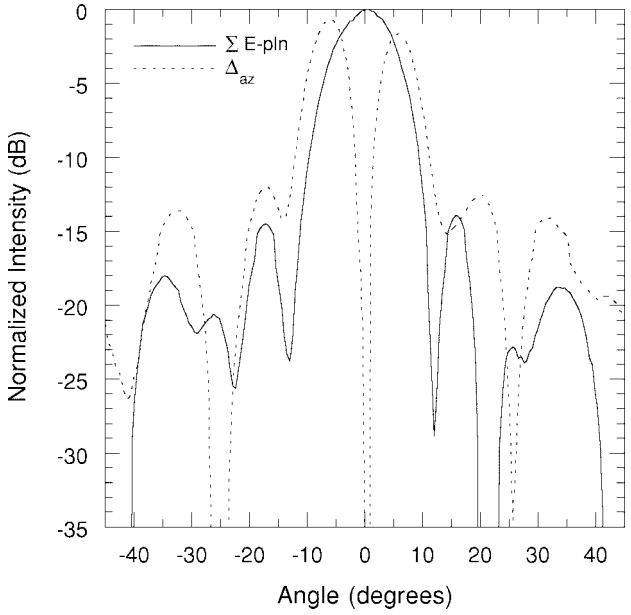

(a)

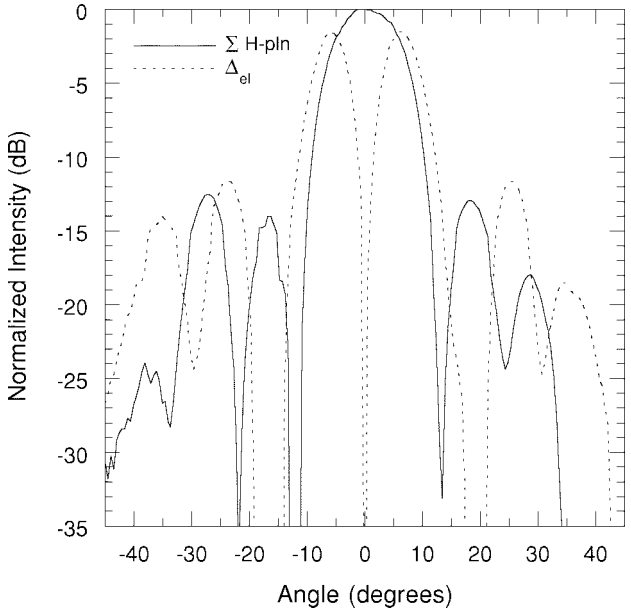

(b)

Fig. 11. Measured monopulse patterns at RF = 93 GHz, IF = 3 GHz: (a) Σ E-plane and Δ_{az} and (b) Σ H-plane and Δ_{el}.

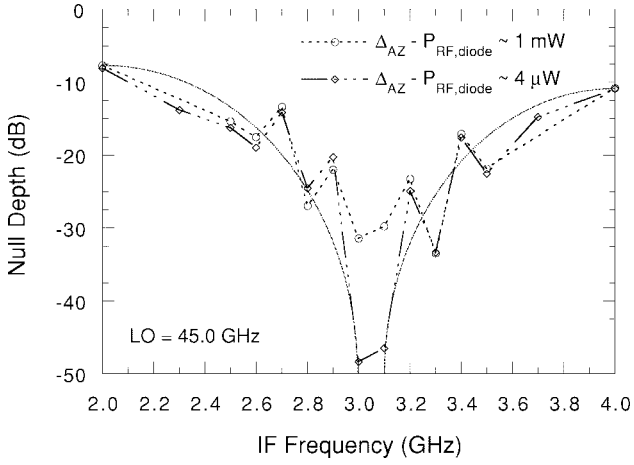

(a)

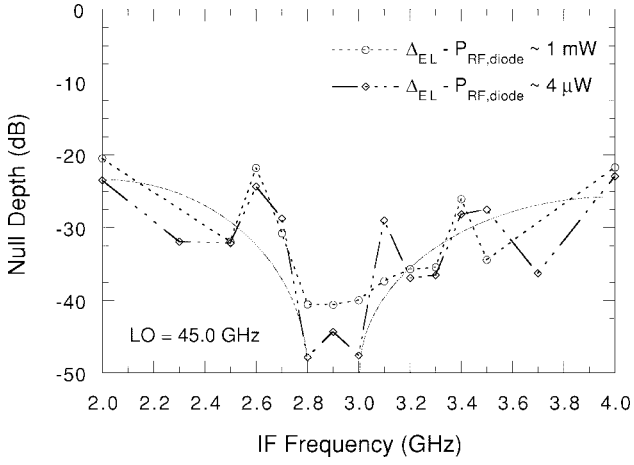

(b)

Fig. 12. Measured difference pattern null depths versus IF frequency with $f_{\rm LO} = 45.0$ GHz. The monopulse comparator is adjusted for the deepest possible null at IF = 3 GHz. (a) Δ_{az} and (b) Δ_{el}. The darker dotted lines show the fitted curves used to estimate the achievable null bandwidths.

TABLE II
ACHIEVABLE NULL BANDWIDTHS

Null (dB)	BW (MHz) Δ_{az}	BW (MHz) Δ_{el}
45	100	200
35	250	600
25	600	2000

Table II summarizes the achievable null bandwidths with the IF monopulse comparator tuned for the maximum null at IF = 3 GHz and the LO held constant at 45.0 GHz. The bandwidths are limited by the IF network (group delay variations from each input port of the comparator to the sum and difference ports brought about by the phase adjustments necessary to maximize the null on boresight at a desired center frequency). The azimuth channel bandwidth is more limited due to the large phase correction needed between the left (channels 1 and 4) and right (channels 2 and 3), resulting in a greater imbalance in the group delays. Wider IF null bandwidths can be achieved by adjusting the phases and amplitudes of the four channels at the expense of the maximum achievable null depth. Wider bandwidths can also be realized by using a Lange-coupler-based monopulse comparator [15]; however, realizing better than 40-dB nulls over a 2-GHz bandwidth will necessitate moving to a higher IF center frequency (perhaps to X-band).

The null depth was also measured versus RF frequency with the IF frequency held constant at 3 GHz (i.e., RF and LO varied together to maintain IF = 3 GHz). First the monopulse network was left tuned for $f_{\rm RF} = 93$ GHz, and the null measurements performed over the indicated range of RF frequencies. Then the monopulse network was retuned for the deepest null possible at each RF frequency of interest. The amount of tuning necessary was relatively small compared to that

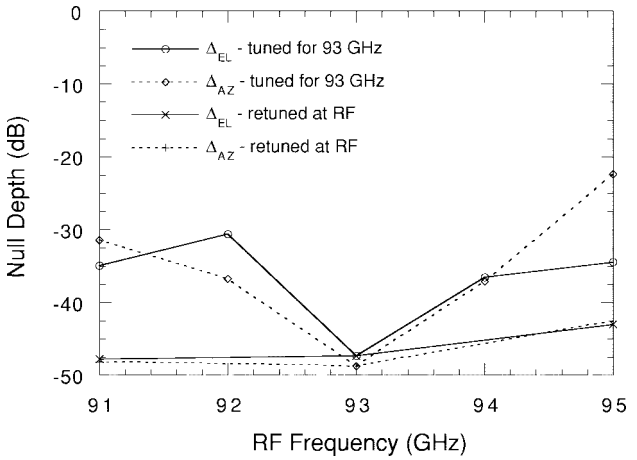

Fig. 13. Measured difference pattern null depths versus RF frequency with IF = 3 GHz.

required when retuning for different IF's. The results of these measurements are shown in Fig. 13. It can be seen that the null depths *without* retuning are below −30 dB in both azimuth and elevation from <91 to 94.5 GHz, and, *with* retuning, the null depth can be maintained better than −42 dB at a wide range of RF frequencies. This demonstrates that the millimeter-wave portions of the monopulse subsystem are able to operate without degradation over at least a 91–95-GHz (5%) bandwidth.

IV. Conclusion and Future Work

An integrated uniplanar monopulse receiver has been realized for operation at W-band frequencies. The receiver is based on a 2 × 2 array of CPW-fed slot-ring antennas feeding an extended hemispherical dielectric lens. The antennas are coupled to uniplanar ×2 subharmonic mixers and the monopulse processing is performed at the IF. Excellent monopulse patterns were measured, with better than 45-dB null depths over a 100–200-MHz bandwidth. This null depth level translates to submilliradian angular accuracy for a 24-mm aperture. 25-dB null depths are possible over a 600-MHz bandwidth. Deep difference pattern nulls were not achieved over the entire 2-GHz bandwidth; the IF monopulse comparator was the limiting factor. However, the receiver was robust with respect to RF frequency. The system noise figure specification (<12 dB) was not met, although the four receiver channels were very well matched with DSB conversion losses of 14.4–14.7 dB at f_{LO} = 45.0 GHz and an estimated LO power of 6–7 dBm available at each mixer.

The following improvements can be made to the receiver design.

- A matching cap layer on the dielectric lens will reduce the front-end losses due to reflections at the lens-air interface, resulting in an improved system noise figure. Furthermore, a semi-insulating GaAs lens, instead of a high-resistivity Si lens, would reduce the absorption loss in the 24 mm lens by approximately 2 dB. However, such a lens would be more expensive and fragile than the Si lens.
- LNA's in the RF path prior to the mixers will set the front-end noise figure (see Section III-A); if the amplifier gain is high enough, the noise figure requirements for the mixers can be relaxed. This would possibly allow the use of ×4 subharmonic mixers, reducing the LO frequency to ∼22.5 GHz and further simplifying the LO distribution network. A CPW × 4 subharmonic mixer design has been developed for this purpose.
- Redesigning the receiver with an on-chip LO would eliminate the need for precision V-connectors and transitions, allowing the LO power to be delivered more efficiently. This would also theoretically minimize the LO phase imbalance between the receiver channels, reducing the amount of phase adjustment necessary in the IF and therefore improving the IF monopulse comparator bandwidth. The Wilkinson power dividers should be redesigned using a larger $w+2g$ to reduce the LO power loss in this component.
- Moving to a higher IF center frequency (for example, 8 GHz) would realistically allow deep (>40 dB) difference pattern nulls to be achieved over a 2-GHz bandwidth with a planar IF monopulse comparator.

A summary of planar millimeter-wave monopulse systems developed to date is presented in Table III. The receiver developed in this work combines many of the advantages of these systems while avoiding some potential limitations. The extended hemispherical dielectric lens approach offers a convenient means of eliminating losses to substrate modes, allowing the millimeter-wave electronics chip to be fabricated on a standard-thickness wafer. The CPW-fed slot-ring antennas are compact, allow for the incorporation of MMIC LNA's in the RF path prior to the downconverters, and offer the potential for polarimetric operation. The uniplanar circuit topology eliminates the need for backside processing and via holes. IF monopulse processing results in deep difference pattern nulls for high-precision angular accuracy. The receiver architecture is readily extended to a dual-polarized configuration; with IF polarization processing, a fully polarimetric monopulse receiver is possible.

The monopulse architecture presented in this paper assumes that the radar target will be illuminated by a separate high-power W-band tube source (e.g., located on the launching platform), and, therefore, does not consider transmit capability. The current design could be extended to a monopulse transceiver with the incorporation of W-band transmit/receive (T/R) MMIC chips in the RF path between the antennas and the mixers; PA/LNA—power amplifier/low noise amplifier—chips are currently under development by industry. It has been shown that the W-band subharmonic mixer design operates effectively as an upconverter as well as a downconverter [10]. One potential drawback is that the available RF transmit power may not be sufficient to provide enough dynamic range to take advantage of the deep monopulse nulls achievable with this receiver.

The integrated monopulse receiver design can also be readily extended to a *fully polarimetric* configuration (Fig. 14). The layout can be visualized as two identical single-polarized monopulse receivers oriented at 90° from each other, but sharing the same antenna elements. The LO feeding must have the same configuration as shown in Fig. 3 for there

TABLE III
SUMMARY OF PLANAR MILLIMETER-WAVE MONOPULSE SYSTEMS DEVELOPED TO DATE. NA INDICATES INFORMATION THAT IS NOT AVAILABLE FROM THE LITERATURE

Organization, Reference	f_0 (GHz)	Array Type[a]	Pol.	Element NF (dB)	Mono. Proc.	Null Depth (dB)[b]	Null Bandwidth	Comments
Northrop-Grumman, [1],[2]	94	FP	CP	NA	RF	~ 20	NA	30 dB receiver gain
Lockheed-Martin/Sanders, [4]	94	PA	LP	7 SSB	RF[c]	~ 20	1.5 GHz	36 dB element gain
Mitsubishi, [3]	100	FP	LP	NA	IF	> 35	NA	Fundamental balanced mixers, C-Band IF
Raytheon, [8]	35	FP	LP	8.7 DSB	IF	30–40	NA	Quasi-optical LO injection, Balanced mixers, L-Band IF
University of Michigan, [5]	94	FP	LP	28-32 SSB	IF	> 35	< 20 MHz	$\times 4$ SHM, 200 MHz IF
This Work	94	FP	LP[d]	14.5 DSB	IF	> 45	100 MHz[e]	$\times 2$ SHM, 2-4 GHz IF

[a]FP = Focal Plane, PA = Phased Array
[b]Relative to *difference* pattern peak.
[c]Monopulse processing performed with waveguide comparator after RF electronics.
[d]Readily extended to a dual-polarized configuration.
[e]See Table II for a more detailed breakdown of achievable null bandwidths.

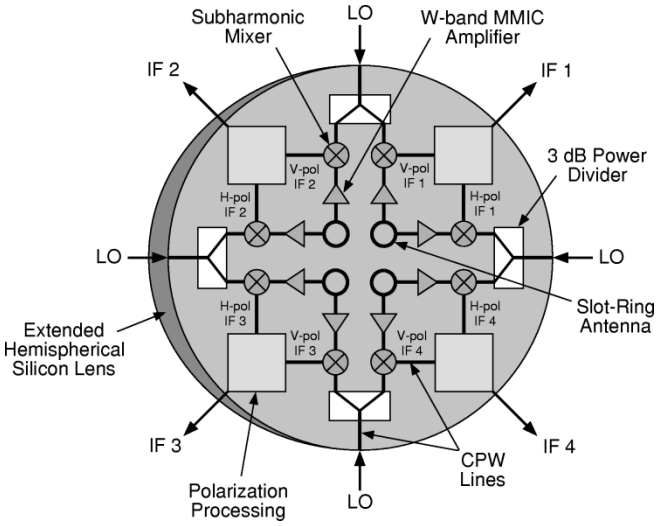

Fig. 14. Conceptual diagram of the integrated millimeter-wave monopulse *polarimetric* receiver design.

to be correct phasing to these "two" orthogonal monopulse receivers. The H-pol and V-pol RF signals from each antenna are mixed down to a corresponding IF. The desired polarization state is identically synthesized from the two IF signals of each antenna, generating four *polarimetric* IF outputs. The polarimetric IF's are then processed as usual in an IF processor. The real vision of the integrated polarimetric monopulse receiver includes these complex IF functions as monolithically realized application-specific integrated circuits (ASIC's). Indeed, a GaAs monolithic monopulse comparator has already been demonstrated consisting of FET-based sum and difference amplifier circuits [16].

Finally, since this monopulse receiver is inherently a staring array, beam steering must be accomplished mechanically with a gimbal mount. An alternative is the use of quasi-optical beam-control grids, currently under investigation by various groups.

ACKNOWLEDGMENT

The authors are particularly indebted to Dr. J. Harvey of the Army Research Office, Electronics Division, for his constant support of the millimeter-wave research effort at the University of Michigan. The authors would also like to thank: Dr. T. W. Crowe of the University of Virginia Semiconductor Device Laboratory, Charlottesville, VA, for providing the high-quality antiparallel diodes; E. Liu of Anritsu/Wiltron, Morgan Hill, CA, for donating the V-connector parts; and S. Shaw of the Naval Surface Warfare Center, Dahlgren Division, and J. Hartranft of The Johns Hopkins University Applied Physics Laboratory for many useful discussions.

REFERENCES

[1] E. C. Niehenke, P. Stenger, T. McCormick, and C. Schwerdt, "A planar 94-GHz transceiver with switchable polarization," in *IEEE 1993 MTT-S Int. Microwave Symp. Dig.*, Atlanta, GA, June 14–18, 1993, pp. 167–170.
[2] H. Fudem *et al.*, "A low cost miniature MMIC W-band transceiver with planar antenna," in *IEEE 1997 MTT-S Int. Microwave Symp. Dig.*, Denver, CO, June 8–13, 1997, pp. 427–430.
[3] A. Iida *et al.*, "A 100 GHz band antenna stacked monolithic receiver for monopulse radar," in *19th Int. Conference on Infrared and Millimeter Waves Dig.*, Oct. 17–20, 1994, pp. 502–503.
[4] J. Sowers *et al.*, "Electronically steered, receive monopulse, active phased array at 94 GHz," in *IEEE 1996 MTT-S Int. Microwave Symp. Dig.*, June 17–21, 1996, pp. 1581–1584.
[5] C. C. Ling and G. M. Rebeiz, "A 94 GHz planar monopulse tracking receiver," *IEEE Trans. Microwave Theory Tech.*, vol. 42, pp. 1863–1871, Oct. 1994.
[6] D. B. Rutledge, D. P. Neikirk, and D. P. Kasilingam, "Integrated-circuit antennas," in *Infrared and Millimeter Waves*, vol. 10, K. J. Button, Ed. New York: Academic, 1983, pp. 1–90.
[7] D. F. Filipovic, S. S. Gearhart, and G. M. Rebeiz, "Double-slot antennas on extended hemispherical and elliptical silicon dielectric lenses," *IEEE Trans. Trans. Microwave Theory Tech.*, vol. 41, pp. 1738–1749, Oct. 1993.
[8] R. L. Gingras *et al.*, "Millimeter-wave slot-ring mixer array receiver technology," in *1992 IEEE MMWMC Symp. Dig.*, June 1992, pp. 105–107.
[9] S. Raman and G. M. Rebeiz, "Single- and dual-polarized millimeter-wave slot-ring antennas," *IEEE Trans. Antennas Propagat.*, vol. 44, pp. 1438–1444, Nov. 1996.
[10] S. Raman, F. Rucky, and G. M. Rebeiz, "A high performance W-band uniplanar subharmonic mixer," *IEEE Trans. Microwave Theory Tech.*, vol. 45, pp. 955–962, June 1997.
[11] F. Brauchler, S. Robertson, J. East, and L. P. B. Katehi, "W-band finite ground coplanar (FGC) line circuit elements," in *IEEE 1996 MTT-S Int. Microwave Symp. Dig.*, June 17–21, 1996, pp. 1845–1848.
[12] J. S. Izadian and S. M. Izadian, *Microwave Transition Design.* Norwood, MA: Artech House, 1988.
[13] C. M. Jackson and J. Newman, "Low cost, Ka-band microstrip patch monopulse antenna," *Microwave J.*, vol. 30, no. 7, pp. 125–131, July 1987.
[14] D.-W. Tu *et al.* "High gain monolithic W-band low noise amplifiers based on pseudomorphic high electron mobility transitors," *IEEE Trans. Microwave Theory Tech.*, vol. 42, no. 12, pp. 2590–2597, Dec. 1994.
[15] N. S. Barker and G. M. Rebeiz, "An octave bandwidth monopulse processor," in *IEEE 1997 MTT-S Int. Microwave Symp. Dig.*, June 8–13, 1997, pp. 405–407.
[16] J. B. Cole *et al.*, "A monolithic monopulse comparator," in *1992 IEEE MMWMC Symp. Dig.*, June 1992, pp. 109–111.

Sanjay Raman (S'84–M'98) was born in Nottingham, U.K., on April 25, 1966. He received the B.E.E. degree (highest honors) from the Georgia Institute of Technology, Atlanta, GA, in 1987, and the M.S.E.E. and Ph.D. degrees from the University of Michigan, Ann Arbor, MI, in 1993 and 1998, respectively.

From 1987 to 1992, he served as a nuclear-trained Submarine Officer in the U.S. Navy. From 1992 to 1998, he was with the EECS Department at the University of Michigan. In January 1998, he joined the faculty of The Bradley Department of Electrical and Computer Engineering, Virginia Polytechnic Institute and State University, Blacksburg, VA, as an Assistant Professor. His research interests include microwave and millimeter-wave circuits and antennas, wireless sensor and communications systems, high-speed/mixed-signal circuits and packaging, micromachining, and solid-state technology.

Dr. Raman received the Best Student Paper Awards at the 1995 IEEE Antennas and Propagation Symposium, Newport Beach, CA, and the 1996 IEEE International Microwave Symposium, San Francisco, CA, and was a cowinner of the 1996 Armed Forces Communications and Electronics Association (AFCEA) postgraduate fellowship. He is a member of ASEE and AFCEA.

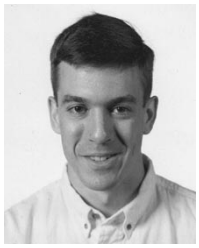

N. Scott Barker (S'95) was born in Angeles City, Philippines, on September 22, 1972. He received the B.S.E.E. degree (High Distinction) from the University of Virginia, Charlottesville, VA, in 1994, and the M.S.E.E degree from the University of Michigan, Ann Arbor, MI, in 1996. He is currently a Ph.D. candidate in electrical engineering at the University of Michigan.

Mr. Barker received a Best Student Paper Award at the 1997 IEEE International Microwave Symposium, Denver, CO.

Gabriel M. Rebeiz (S'86–M'88–SM'93–F'97), for biography, see this issue, p. 2288.